

# MAXIMUM-ENTROPY-BASED TOMOGRAPHIC RECONSTRUCTION OF BEAM DENSITY DISTRIBUTION\*

Y.-N. Rao, R. Baartman, TRIUMF, Vancouver, Canada

I. Tashev, UBC, Vancouver, Canada

G. Goh, SFU, Burnaby, Canada

## Abstract

For ISAC at TRIUMF, radioactive isotopes are generated with a 500 MeV proton beam. The beam power is up to 40 kW and can easily melt the delicate target if too tightly focused. We protect this target by closely monitoring the distribution of the incident proton beam. There is a 3-wire scanner monitor installed near the target; these give the vertical profile and the  $+45^\circ$  and  $-45^\circ$  profiles. Our objective is to use these 3 measured projections to find the 2-D density distribution. By implementing the maximum entropy (MENT) algorithm, we have developed a computer program to realize tomographic reconstruction of the beam density distribution. Of particular concern is to make the calculation sufficiently efficient such that an operator can obtain the distribution within a few seconds of the scan. As well, we have developed the technique to perform phase space reconstruction, using many wire scans and the calculated transfer matrices between them. In this paper we present details of the computer code and the techniques used to improve noise tolerance and compute efficiency, after reviewing the MENT algorithm.

## MAXIMUM ENTROPY TOMOGRAPHY

Tomographic reconstruction algorithms offer the possibility to reconstruct higher dimensional density distribution from a series of projections measured in a lower dimensional subspace. In the absence of a large number of projections, the Maximum Entropy (MENT) algorithm [1] can reconstruct a distribution that maximizes the entropy and simultaneously reproduces all the measured projections exactly. In other words, MENT can find a most probable solution with minimized artifacts to describe the observed data. This has proven to be superior in the case where there are only a few projections available.

We will only be dealing with 2-D distribution here. Let  $f(x, y)$  be the source distribution. It satisfies

$$f(x, y) \geq 0 \text{ and } \int \int f(x, y) dx dy = 1 \quad (1)$$

The projection  $P(x)$  of this distribution on the  $x$ -axis is defined by

$$P(x) = \int_{-\infty}^{+\infty} f(x, y) dy \quad (2)$$

The input data for tomographic reconstruction is a set of such projections onto  $N$  different  $s$ -axes defined by a set

of transformation matrices  $R_i$  ( $i = 1, 2, \dots, N$ ):

$$\begin{pmatrix} s \\ t \end{pmatrix} = R_i \begin{pmatrix} x \\ y \end{pmatrix} = \begin{pmatrix} a & b \\ c & d \end{pmatrix}_i \begin{pmatrix} x \\ y \end{pmatrix} \quad (3)$$

The transformation matrix  $R_i$  can be a rotation matrix, used for real space reconstruction, or the beam transport matrices for reconstruction of phase space density. It conserves the area of the source distribution because  $\det(R_i) = 1$ . Using the inverse transformation from the  $i^{\text{th}}$  projection coordinates  $(s, t)$  back to the  $(x, y)$  source plane, the  $i^{\text{th}}$  projection is represented as

$$P_i(s) = \int_{-\infty}^{+\infty} f[x_i(s, t), y_i(s, t)] dt \quad (4)$$

The goal is to invert Eq. 4 and determine the function  $f(x, y)$ . However, the inversion is not unique unless the number of projections  $N$  is infinite. For a finite number of measurements, many different distributions exist that can reproduce all the measured projections. Out of these distributions, the one that maximizes the entropy

$$E(f) = - \int_{-\infty}^{+\infty} \int_{-\infty}^{+\infty} f(x, y) \ln f(x, y) dx dy \quad (5)$$

and satisfies the boundary conditions of Eq. 4 is the most appropriate one, because it contains the least information.

The extended entropy function, with boundary conditions, can be written as

$$\varepsilon(f, \lambda) = E(f) - \sum_{i=1}^N \int_{-\infty}^{+\infty} \lambda_i(s) [f(x_i, y_i) dt - P_i] ds \quad (6)$$

where  $x_i$  and  $y_i$  are functions of  $s, t$ , and where the  $\lambda_i(s)$  denotes the Lagrange multiplier functions. The conditions for the stationary solution are

$$\frac{\partial \varepsilon(f, \lambda)}{\partial \lambda_i} = 0 \text{ and } \frac{\partial \varepsilon(f, \lambda)}{\partial f} = 0 \quad (7)$$

The first condition in Eq. 7 is in fact equivalent to the constraints defined by Eq. 4, whereas the second one gives

$$\ln[f(x, y)] = \sum_{i=1}^N \lambda_i - 1 \text{ or } f(x, y) = \prod_{i=1}^N H_i \quad (8)$$

where the unknown Lagrange multipliers  $\lambda_i$  have been replaced by the equally unknown functions  $H_i = \exp(\lambda_i - 1/N)$ . The arguments of these functions are  $s_i = a_i x + b_i y$ , completely determined by the projection. So, the task is merely to find these  $H$ -values for the equation.

\* TRIUMF receives funding via a contribution agreement through the National Research Council of Canada.

Since the measured projections are received as discrete rather than continuous distributions, it's natural to formulate a binned projection as following

$$G_{ij} = \int_{s_{ij}}^{s_{i(j+1)}} P_i(s) ds = \int_{-\infty}^{+\infty} \int_{-\infty}^{+\infty} f(x, y) \Gamma_{ij} dx dy \quad (9)$$

where  $\Gamma_{ij}$  denotes a characteristic function

$$\Gamma_{ij}(s) = \begin{cases} 1 & s_{ij} \leq s \leq s_{i(j+1)} \\ 0 & \text{otherwise} \end{cases} \quad (10)$$

Therefore, Eq. 8 can be written as

$$f(x, y) = \prod_{i=1}^N \sum_{j=1}^{M_i} H_{ij} \Gamma_{ij} \quad (11)$$

Substituting Eq. 11 in Eq. 9 gives an iteration relation for the factors  $H_{ij}$

$$H_{ij} = \frac{G_{ij}}{\int \int dx dy \Gamma_{ij} \left\{ \prod_{k \neq i}^N \sum_{l=1}^{M_k} H_{kl} \Gamma_{kl} \right\}} \quad (12)$$

After the  $H$ -factors are computed, they can be substituted back into Eq. 8 to compute the distribution function  $f(x, y)$ .

## COMPUTER PROGRAM

We implemented the MENT algorithm and developed a computer program [2][3] in C/C++ at TRIUMF from scratch to accomplish tomographic reconstruction of beam density distribution. Our program is stand-alone, independent of any external libraries. Of particular concern is to make the program robust and sufficiently efficient such that one can obtain the distribution within a few seconds of the scan. First of all, the conditions defined in Eq. 1 imply that the input projection profiles must have non-negative background and must be normalized to one, namely,  $G_{ij} \geq 0$  and  $\sum_{j=1}^{M_i} G_{ij} = 1$ . However, the input data are usually noisy, and even spiky and also inconsistent in terms of the intensities from different projections. Therefore, it's crucial to pre-process the data before feeding them into the MENT routine.

### Data Pre-processing

Data pre-processing is composed of two major steps in our program: statistics calculation and FFT smoothing. In details:

- Calculate the 2rms size  $T$  and centroid  $C$  so as to determine a proper window for efficient smoothing with FFT. Only the data within a window between  $C - 2T$  and  $C + 2T$  are retained for next use; everything outside is discarded.  $C$  and  $T$  are calculated by sampling an area with no signal to determine offset and 2rms noise, subtracting the offset, cutting off the 2rms noise

level in the background and then removing isolated spikes. But in this step, we actually do not make any changes (subtraction or cut) to the data in the retained window.

- Do FFT to smooth the retained data using a low-pass filter. The cut-off frequency of the filter is one of the input parameters that is allowed to change by the user. The profile after being smoothed may still have non-zero offset and wiggles in the background. So, next we subtract this offset and then make a 2rms cut to zero off everything in the background. This results in a clean profile with zero background to pass on to the MENT function for tomographic reconstruction. However, the noisier the data, the more of the distribution tails will be unavoidably deleted.

### Test Runs

One of the test runs [3] we made was specifically related to the profile monitor near the ISAC target, which measures only three projections:  $\pm 45^\circ$  and vertical. This example deals with a distribution of a Gaussian core plus an asymmetric halo, moreover, this Gaussian core is tall and narrow: the vertical rms size is 3 times the horizontal one. The reconstruction from the 3 profiles gives distribution function  $f(x, y)$  correct to within 15% (standard deviation). This is shown in Fig. 1.

Another test was for phase space reconstruction, related to the measurements in the TRIUMF injection line. In this test, we used a crescent shape to represent the initial phase space of beam, instead of a regular elliptical shape. This phase space was transformed through a quadrupole to a location downstream. For a specified quad setting, a profile was obtained from projection on the  $x$ -axis. There were 12 profiles simulated; these, along with the corresponding transfer matrices, were fed into the MENT program to reconstruct the initial phase space. Fig. 2 shows the result. The crescent shape is very well reproduced. Also, an important conclusion from this exercise is that in order to reveal the crescent result, the phase advance between the source point and the observation point must be made large enough, i.e.  $\geq 90^\circ$ , and over this  $\geq 90^\circ$  phase advance, the more projections one uses, the more precise reconstruction result one can achieve.

## APPLICATIONS

Our program has been incorporated into the cyclotron and beamline central control computer to accomplish on-line monitoring of the beam distribution near the ISAC target. Within  $\sim 5$  seconds of a scan, an operator can obtain the result. Fig. 3 is an example snapshot, showing the 3 projections measured and the reconstructed 2-D contour plot and H, V distributions.

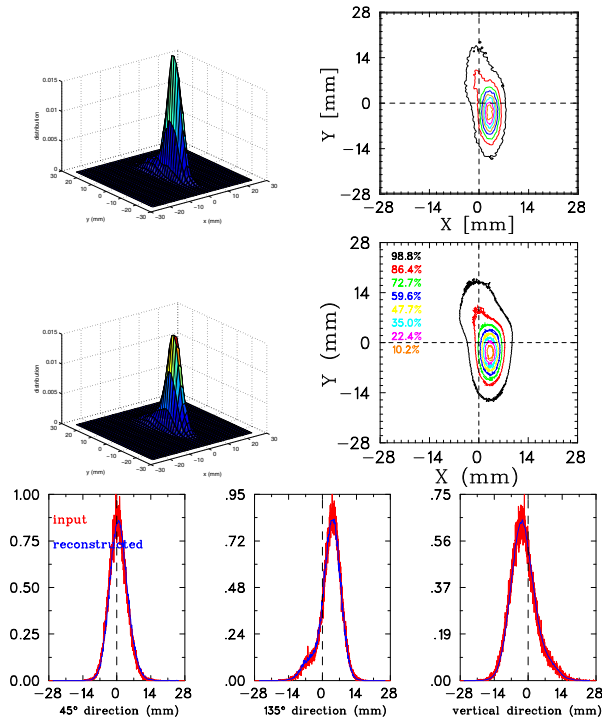


Figure 1: Illustration of the first test made to the tomography program for the real space reconstruction, using a narrow Gaussian core plus an asymmetric halo as is shown on top as 3-D surface plot (left) and contour plot (right). The reconstructed result is shown in the middle. The 3 projections that were fed into the program and reconstructed from the program are shown at bottom.

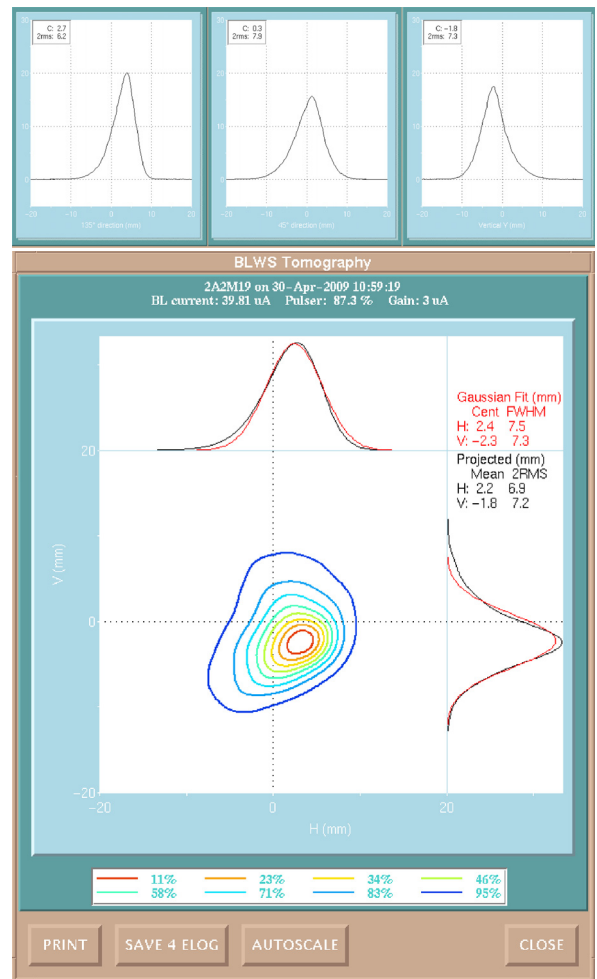


Figure 3: A snapshot of MENT program online application, displaying the 3 measured projections and the reconstructed 2-D contour plot and H,V distributions.

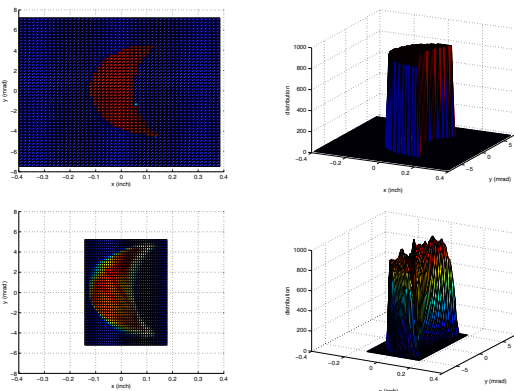


Figure 2: Illustration of the second test made for the phase space reconstruction, using a crescent shaped initial phase space as is shown on top as surface plots. The reconstructed result is shown at bottom. Here the phase advance is  $> 90^\circ$  between the source location and the observation location.

**ACKNOWLEDGMENTS**

The authors would like to thank J. Scheins from FZ-Juelich and F. Loehl from DESY for kindly providing their MENT code.

**REFERENCES**

- [1] G. Minerbo, *MENT: A Maximum Entropy Algorithm for Reconstructing a Source from Projection Data*, COMPUTER GRAPHICS AND IMAGE PROCESSING, **10**, 48-68(1979).
- [2] J.J. Scheins, *Tomographic Reconstruction of Transverse and Longitudinal Phase Space Distribution using the Maximum Entropy Algorithm*, TESLA Report 2004-08, 2004.
- [3] Ivan Tashev, Y.-N. Rao, R. Baartman, *Program for Tomographic Reconstruction of Beam Distribution in Real Space*, TRIUMF Design Note TRI-DN-07-29, October 17, 2007.